

Quantum numbers of the $X(3872)$ state and orbital angular momentum in its $\rho^0 J/\psi$ decay

R. Aaij *et al.*^{*}

(LHCb Collaboration)

(Received 23 April 2015; published 30 July 2015)

Angular correlations in $B^+ \rightarrow X(3872)K^+$ decays, with $X(3872) \rightarrow \rho^0 J/\psi$, $\rho^0 \rightarrow \pi^+\pi^-$ and $J/\psi \rightarrow \mu^+\mu^-$, are used to measure orbital angular momentum contributions and to determine the J^{PC} value of the $X(3872)$ meson. The data correspond to an integrated luminosity of 3.0 fb^{-1} of proton-proton collisions collected with the LHCb detector. This determination, for the first time performed without assuming a value for the orbital angular momentum, confirms the quantum numbers to be $J^{PC} = 1^{++}$. The $X(3872)$ is found to decay predominantly through an S wave and an upper limit of 4% at 95% C.L. is set on the D-wave contribution.

DOI: 10.1103/PhysRevD.92.011102

PACS numbers: 13.25.Hw, 13.25.Gv, 14.40.Nd, 14.40.Rt

The $X(3872)$ state was discovered in $B^{+,0} \rightarrow X(3872)K^{+,0}$, $X(3872) \rightarrow \pi^+\pi^-J/\psi$, $J/\psi \rightarrow \ell^+\ell^-$ decays by the Belle experiment [1] and subsequently confirmed by other experiments [2–4].¹ Its production was also studied at the LHC [5,6]. However, the nature of this state remains unclear. The $X(3872)$ state is narrow, has a mass very close to the $D^0\bar{D}^{*0}$ threshold and decays to $\rho^0 J/\psi$ and $\omega J/\psi$ final states with comparable branching fractions [7], thus violating isospin symmetry. This suggests that the $X(3872)$ particle may not be a simple $c\bar{c}$ state, and exotic states such as $D^0\bar{D}^{*0}$ molecules [8], tetraquarks [9] or mixtures of states [10] have been proposed to explain its composition. The $X(3872)$ quantum numbers, such as total angular momentum J , parity P and charge conjugation C , impose constraints on the theoretical models of this state. The orbital angular momentum L in the $X(3872)$ decay may also provide information on its internal structure.

Observations of the $X(3872) \rightarrow \gamma J/\psi$ and $X(3872) \rightarrow \gamma\psi(2S)$ decays [11–13] imply positive C , which requires the total angular momentum of the dipion system ($J_{\pi\pi}$) in $X(3872) \rightarrow \pi^+\pi^-J/\psi$ decays to be odd. The dipion mass, $M(\pi^+\pi^-)$, is limited by the available phase space to be less than 775 MeV, and so $J_{\pi\pi} \geq 3$ can be ruled out since there are no known or predicted mesons with such high spins at such low masses.² In fact, the distribution of $M(\pi^+\pi^-)$ is consistent with $X(3872) \rightarrow \rho^0 J/\psi$ decays [6,14,15], in line with $J_{\pi\pi} = 1$, the only plausible value.

The choices for J^{PC} were narrowed down to two possibilities, 1^{++} or 2^{-+} , by the CDF Collaboration, via an analysis of the angular correlations in inclusively reconstructed $X(3872) \rightarrow \pi^+\pi^-J/\psi$ and $J/\psi \rightarrow \mu^+\mu^-$ decays, dominated by prompt production in $p\bar{p}$ collisions [16]. Using 1.0 fb^{-1} of pp collision data collected by LHCb, $J^{PC} = 2^{-+}$ was ruled out in favor of the 1^{++} assignment, using the angular correlations in the same decay chain, with the $X(3872)$ state produced in $B^+ \rightarrow X(3872)K^+$ decays [17]. Both angular analyses assumed that the lowest orbital angular momentum between the $X(3872)$ decay products (L_{\min}) dominated the matrix element. Significant contributions from $L_{\min} + 2$ amplitudes could invalidate the 1^{++} assignment. Since the phase-space limit on $M(\pi^+\pi^-)$ is close to the ρ^0 pole (775.3 ± 0.3 MeV [7]), the energy release in the $X(3872)$ decay, $Q \equiv M(J/\psi\pi^+\pi^-) - M(J/\psi) - M(\pi^+\pi^-)$, is a small fraction of the $X(3872)$ mass, making the orbital angular momentum barrier effective.³ However, an exotic component in $X(3872)$ could induce contributions from higher orbital angular momentum for models in which the size of the $X(3872)$ state is substantially larger than the compact sizes of the charmonium states. Therefore, it is important to probe the $X(3872)$ spin-parity without any assumptions about L . A determination of the magnitude of contributions from $L_{\min} + 2$ amplitudes for the correct J^{PC} is also of interest, since a substantial value would suggest an anomalously large size of the $X(3872)$ state. In this article, we extend our previous analysis [17] of five-dimensional angular correlations in $B^+ \rightarrow X(3872)K^+$, $X(3872) \rightarrow \rho^0 J/\psi$, $\rho^0 \rightarrow \pi^+\pi^-$, $J/\psi \rightarrow \mu^+\mu^-$ decays to accomplish these goals. The integrated luminosity of the data sample has been tripled by adding 8 TeV pp collision data collected in 2012.

^{*}Full author list given at the end of the article.

¹The inclusion of charge-conjugate states is implied in this article.

²We use mass and momentum units in which $c = 1$.

Published by the American Physical Society under the terms of the Creative Commons Attribution 3.0 License. Further distribution of this work must maintain attribution to the author(s) and the published article's title, journal citation, and DOI.

³Dimuon candidates are constrained to the known J/ψ mass [7].

The LHCb detector is a single-arm forward spectrometer covering the pseudorapidity range $2 < \eta < 5$, described in detail in Refs. [18,19]. The $X(3872)$ candidate selection, which is based on reconstructing $B^+ \rightarrow (J/\psi \rightarrow \mu^+ \mu^-) \pi^+ \pi^- K^+$ candidates using particle identification information and transverse momentum (p_T) thresholds and requiring separation of tracks and the B^+ vertex from the primary pp interaction vertex, is improved relative to that of Ref. [17]. The signal efficiency is increased by lowering requirements on p_T for muons from 0.90 to 0.55 GeV and for hadrons from 0.25 to 0.20 GeV. The background is further suppressed without significant loss of signal by requiring $Q < 250$ MeV. The $X(3872)$ mass resolution ($\sigma_{\Delta M}$) is improved from about 5.5 to 2.8 MeV by constraining the B^+ candidate to its known mass and requiring its momentum to point to a pp collision vertex in the kinematic fit of its decay. The distribution of $\Delta M \equiv M(\pi^+ \pi^- J/\psi) - M(J/\psi)$ is shown in Fig. 1. A Crystal Ball function [20] with symmetric tails is used to model the signal shape, while the background is assumed to be linear. An unbinned maximum-likelihood fit yields 1011 ± 38 $B^+ \rightarrow X(3872)K^+$ decays and 1468 ± 44 background entries in the $725 < \Delta M < 825$ MeV range used in the angular analysis. The signal purity is 80% within $2.5\sigma_{\Delta M}$ from the signal peak. From studying the $K^+ \pi^+ \pi^-$ mass distribution, the dominant source of the background is found to be $B^+ \rightarrow J/\psi K_1(1270)^+$, $K_1(1270)^+ \rightarrow K^+ \pi^+ \pi^-$ decays.

Angular correlations in the B^+ decay chain are analyzed using an unbinned maximum-likelihood fit to determine the $X(3872)$ quantum numbers and orbital angular momentum in its decay. The probability density function (\mathcal{P}) for each J^{PC} hypothesis, J_X , is defined in the five-dimensional angular space $\Omega \equiv (\cos \theta_X, \cos \theta_\rho, \Delta \phi_{X,\rho}, \cos \theta_{J/\psi}, \Delta \phi_{X,J/\psi})$,

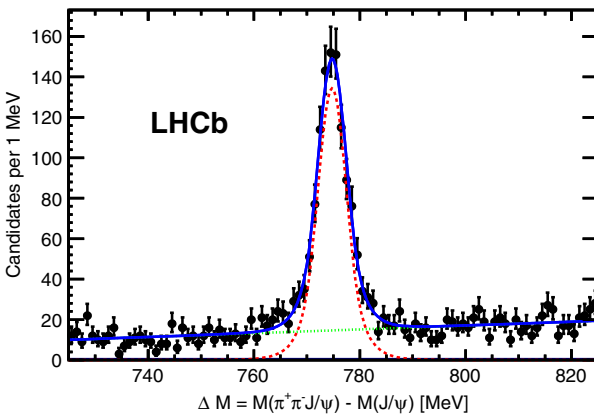


FIG. 1 (color online). Distribution of ΔM for $B^+ \rightarrow J/\psi K^+ \pi^+ \pi^-$ candidates. The fit of the $X(3872)$ signal is displayed. The solid (blue), dashed (red) and dotted (green) lines represent the total fit, signal component and background component, respectively.

where θ_X , θ_ρ and $\theta_{J/\psi}$ are the helicity angles [21–23] in the $X(3872)$, ρ^0 and J/ψ decays, respectively, and $\Delta \phi_{X,\rho}$, $\Delta \phi_{X,J/\psi}$ are the angles between the decay planes of the $X(3872)$ particle and of its decay products. The quantity \mathcal{P} is the normalized product of the expected decay matrix element (\mathcal{M}) squared and of the reconstruction efficiency (ϵ), $\mathcal{P}(\Omega|J_X) = |\mathcal{M}(\Omega|J_X)|^2 \epsilon(\Omega)/I(J_X)$, where $I(J_X) = \int |\mathcal{M}(\Omega|J_X)|^2 \epsilon(\Omega) d\Omega$. The efficiency is averaged over the $\pi^+ \pi^-$ mass using a simulation [24–28] of the $X(3872) \rightarrow \rho^0 J/\psi$, $\rho^0 \rightarrow \pi^+ \pi^-$ decay. The line shape of the ρ^0 resonance can change slightly depending on the $X(3872)$ spin hypothesis. The effect on $\epsilon(\Omega)$ is very small and is neglected. The angular correlations are obtained using the helicity formalism [16],

$$|\mathcal{M}(\Omega|J_X)|^2 = \sum_{\Delta \lambda_\mu = -1,+1} \left| \sum_{\lambda_{J/\psi}, \lambda_\rho = -1,0,+1} A_{\lambda_{J/\psi}, \lambda_\rho} D_{0, \lambda_{J/\psi} - \lambda_\rho}^{J_X}(0, \theta_X, 0)^* D_{\lambda_\rho, 0}^1(\Delta \phi_{X,\rho}, \theta_\rho, 0)^* D_{\lambda_{J/\psi}, \Delta \lambda_\mu}^1(\Delta \phi_{X,J/\psi}, \theta_{J/\psi}, 0)^* \right|^2, \quad (1)$$

where the λ 's are particle helicities, $\Delta \lambda_\mu = \lambda_{\mu^+} - \lambda_{\mu^-}$ and $D_{\lambda_1, \lambda_2}^J$ are Wigner functions [21–23]. The helicity couplings, $A_{\lambda_{J/\psi}, \lambda_\rho}$, are expressed in terms of the LS couplings, B_{LS} , with the help of Clebsch-Gordan coefficients, where L is the orbital angular momentum between the ρ^0 and the J/ψ mesons, and S is the sum of their spins,

$$A_{\lambda_{J/\psi}, \lambda_\rho} = \sum_L \sum_S B_{LS} \begin{pmatrix} J_{J/\psi} & J_\rho \\ \lambda_{J/\psi} & -\lambda_\rho \end{pmatrix} \begin{pmatrix} S \\ \lambda_{J/\psi} - \lambda_\rho \end{pmatrix} \times \begin{pmatrix} L & S \\ 0 & \lambda_{J/\psi} - \lambda_\rho \end{pmatrix} \begin{pmatrix} J_X \\ \lambda_{J/\psi} - \lambda_\rho \end{pmatrix}. \quad (2)$$

Possible values of L are constrained by parity conservation, $P_X = P_{J/\psi} P_\rho (-1)^L = (-1)^L$. In the previous analyses [14,16,17], only the minimal value of the angular momentum, L_{\min} , was allowed. Thus, for the preferred $J^{PC} = 1^{++}$ hypothesis, the D wave was neglected allowing only S -wave decays. In this work all L values are allowed in Eq. (2). The corresponding B_{LS} amplitudes are listed in Table I. Values of J_X up to 4 are analyzed. Since the orbital angular momentum in the B^+ decay equals J_X , high values are suppressed by the angular momentum barrier. In fact, the highest observed spin of any resonance produced in B decays is 3 [29,30]. Since \mathcal{P} is insensitive to the overall normalization of the B_{LS} couplings and to the phase of the matrix element, the B_{LS} amplitude with the lowest L and S is set to the arbitrary reference value (1,0). The set of other possible complex B_{LS} amplitudes, which are free parameters in the fit, is denoted as α .

QUANTUM NUMBERS OF THE $X(3872)$ STATE AND ...

TABLE I. Parity-allowed LS couplings in the $X(3872) \rightarrow \rho^0 J/\psi$ decay. For comparison, we also list a subset of these couplings corresponding to the lowest L , used in the previous determinations [14,16,17] of the $X(3872)$ quantum numbers.

J^{PC}	B_{LS}	
	Any L value	Minimal L value
0^{-+}	B_{11}	B_{11}
0^{++}	B_{00}, B_{22}	B_{00}
1^{-+}	$B_{10}, B_{11}, B_{12}, B_{32}$	B_{10}, B_{11}, B_{12}
1^{++}	B_{01}, B_{21}, B_{22}	B_{01}
2^{-+}	$B_{11}, B_{12}, B_{31}, B_{32}$	B_{11}, B_{12}
2^{++}	$B_{02}, B_{20}, B_{21}, B_{22}, B_{42}$	B_{02}
3^{-+}	$B_{12}, B_{30}, B_{31}, B_{32}, B_{52}$	B_{12}
3^{++}	$B_{21}, B_{22}, B_{41}, B_{42}$	B_{21}, B_{22}
4^{-+}	$B_{31}, B_{32}, B_{51}, B_{52}$	B_{31}, B_{32}
4^{++}	$B_{22}, B_{40}, B_{41}, B_{42}, B_{62}$	B_{22}

The function to be minimized is $-2 \ln \mathcal{L}(J_X, \alpha) \equiv -s_w 2 \sum_{i=1}^{N_{\text{data}}} w_i \ln \mathcal{P}(\Omega_i | J_X, \alpha)$, where $\mathcal{L}(J_X, \alpha)$ is the unbinned likelihood, and N_{data} is the number of selected candidates. The background is subtracted using the *sPlot* technique [31] by assigning a weight, w_i , to each candidate based on its ΔM value (see Fig. 1). No correlations between ΔM and Ω are observed. Prompt production of $X(3872)$ in pp collisions gives negligible contribution to the selected sample. Statistical fluctuations in the background subtraction are taken into account in the log-likelihood value via a constant scaling factor, $s_w = \sum_{i=1}^{N_{\text{data}}} w_i / \sum_{i=1}^{N_{\text{data}}} w_i^2$. The efficiency $\epsilon(\Omega)$ is not determined on an event-by-event basis, since it cancels in the likelihood ratio except for the normalization integrals. A large sample of simulated events, with uniform angular distributions, passed through a full simulation of the detection and the data selection process, is used to carry out the integration, $I(J_X) \propto \sum_{i=1}^{N_{\text{MC}}} |\mathcal{M}(\Omega_i | J_X)|^2$, where N_{MC} is the number of reconstructed simulated events. The negative log likelihood is minimized for each J_X value with respect to free B_{LS} couplings, yielding their estimated set of values $\hat{\alpha}$. Hereinafter, $\mathcal{L}(J_X) \equiv \mathcal{L}(J_X, \hat{\alpha})$.

The 1^{++} hypothesis gives the highest likelihood value. From angular momentum and parity conservation, there are two possible values of orbital angular momentum in the $X(3872)$ decay for this J^{PC} value, $L = 0$ or 2 . For the S-wave decay, the total spin of the ρ^0 and J/ψ mesons must be $S = 1$; thus B_{01} is the only possible LS amplitude. For the D-wave decay, two values are possible, $S = 1$ or 2 , corresponding to the amplitudes B_{21} and B_{22} , respectively. The squared magnitudes of both of these D-wave amplitudes are consistent with zero, as demonstrated by the ratios $|B_{21}|^2 / |B_{01}|^2 = 0.002 \pm 0.004$ and $|B_{22}|^2 / |B_{01}|^2 = 0.007 \pm 0.008$. Overall, the D-wave significance is only 0.8 standard deviations as obtained by applying Wilks theorem to the ratio of the likelihood values with the D-wave amplitudes floated in the fit and with them fixed to zero.

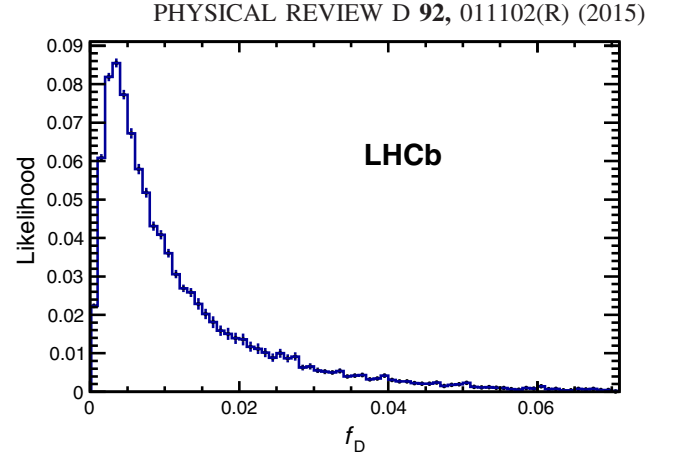


FIG. 2 (color online). Likelihood-weighted distribution of the D-wave fraction. The distribution is normalized to unity.

The total D-wave fraction depends on the B_{LS} amplitudes, $f_D \equiv \int |\mathcal{M}(\Omega)_D|^2 d\Omega / \int |\mathcal{M}(\Omega)_{S+D}|^2 d\Omega$, where $\mathcal{M}(\Omega)_D$ is the matrix element restricted to the B_{21} and B_{22} amplitudes only and $\mathcal{M}(\Omega)_{S+D}$ is the full matrix element. To set an upper limit on f_D , we populate the four-dimensional space of complex B_{21} and B_{22} parameters

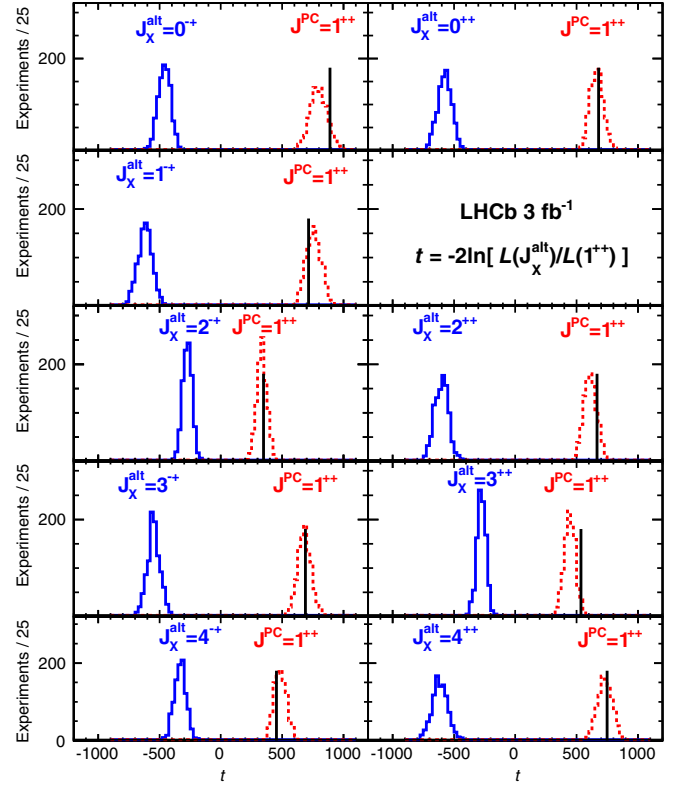


FIG. 3 (color online). Distributions of the test statistic $t \equiv -2 \ln [\mathcal{L}(J_X^{\text{alt}}) / \mathcal{L}(1^{++})]$, for the simulated experiments under the $J^{PC} = J_X^{\text{alt}}$ hypothesis (blue solid histograms) and under the $J^{PC} = 1^{++}$ hypothesis (red dashed histograms). The values of the test statistics for the data, t_{data} , are shown by the solid vertical lines.

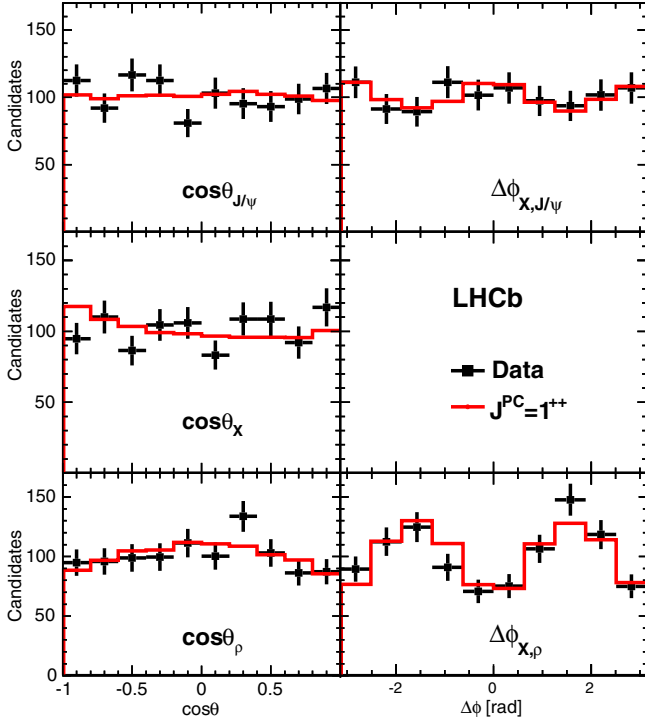


FIG. 4 (color online). Background-subtracted distributions of all angles for the data (points with error bars) and for the 1^{++} fit projections (solid histograms).

with uniformly distributed points in a large region around the B_{21} and B_{22} fit values (± 14 standard deviations in each parameter). For each point we determine the likelihood value from the data and an f_D value via numerical integration of the matrix element squared. The distribution of f_D values weighted by the likelihood values is shown in Fig. 2. It peaks at 0.4% with a non-Gaussian tail at higher values. An upper limit of $f_D < 4\%$ at 95% C.L. is determined using a Bayesian approach.

The likelihood ratio $t \equiv -2 \ln[\mathcal{L}(J_X^{\text{alt}})/\mathcal{L}(1^{++})]$ is used as a test variable to discriminate between the 1^{++} and alternative spin hypotheses considered (J_X^{alt}). The values of t in the data (t_{data}) are positive, favoring the 1^{++} assignment. They are incompatible with the distributions of t observed in experiments simulated under various J_X^{alt} hypotheses, as illustrated in Fig. 3. To quantify these disagreements we calculate the approximate significance of rejection (the p-value) of J_X^{alt} as $(t_{\text{data}} - \langle t \rangle)/\sigma(t)$, where $\langle t \rangle$ and $\sigma(t)$ are the mean and rms deviations of the t distribution under the J_X^{alt} hypothesis. In all spin configurations tested, we exclude the alternative spin hypothesis with a significance of more than 16 standard deviations. Values of t in data are consistent with those expected in the 1^{++} case as shown in Fig. 3, with fractions of simulated 1^{++} experiments with $t < t_{\text{data}}$ in the 25%–91% range. Projections of the data and of the fit \mathcal{P} onto individual angles show good consistency with the 1^{++} assignment as

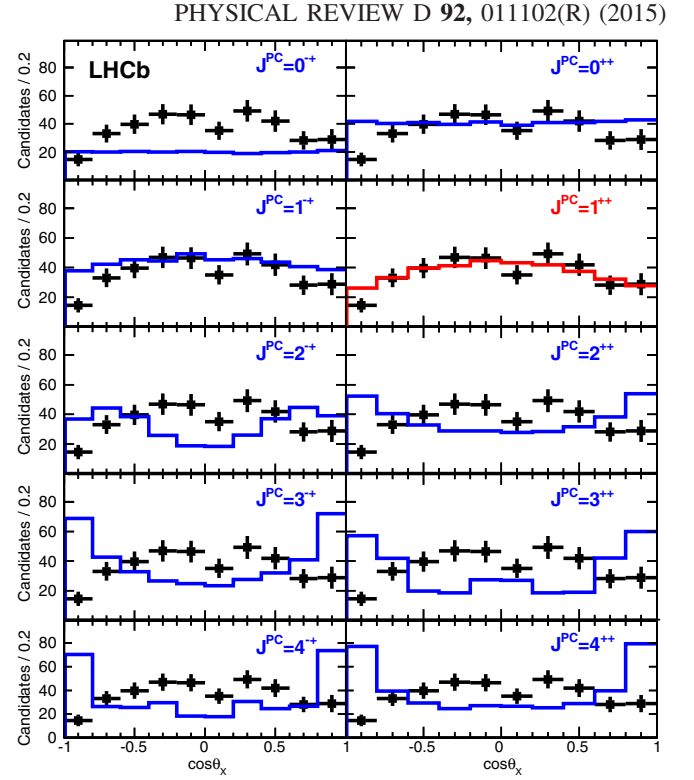


FIG. 5 (color online). Background-subtracted distribution of $\cos\theta_X$ for candidates with $|\cos\theta_p| > 0.6$ for the data (points with error bars) compared to the expected distributions for various $X(3872)$ J^{PC} assignments (solid histograms) with the B_{LS} amplitudes obtained by the fit to the data in the five-dimensional angular space. The fit displays are normalized to the observed number of the signal events in the full angular phase space.

illustrated in Fig. 4. Inconsistency with the other assignments is apparent when correlations between various angles are exploited. For example, the data projection onto $\cos\theta_X$ is consistent only with the 1^{++} fit projection after requiring $|\cos\theta_p| > 0.6$ (see Fig. 5), while inconsistency with the other quantum number assignments is less clear without the $\cos\theta_p$ requirement.

The selection criteria are varied to probe for possible biases from the background subtraction and the efficiency corrections. By requiring $Q < 0.1$ GeV, the background level is reduced by more than a factor of 2, while losing only 20% of the signal. By tightening the requirements on the p_T of the π , K and μ candidates, we decrease the signal efficiency by around 75% with a similar reduction in the background level. In all cases, the significance of the rejection of the disfavored hypotheses is compatible with that expected from the simulation. Likewise, the best fit f_D values determined for these subsamples of data change within the expected statistical fluctuations and remain consistent with the upper limit we have set.

In summary, the analysis of the angular correlations in $B^+ \rightarrow X(3872)K^+$, $X(3872) \rightarrow \pi^+\pi^-J/\psi$, $J/\psi \rightarrow \mu^+\mu^-$ decays, performed for the first time without any assumption about the orbital angular momentum in the $X(3872)$ decay,

QUANTUM NUMBERS OF THE $X(3872)$ STATE AND ...

confirms that the eigenvalues of total angular momentum, parity and charge conjugation of the $X(3872)$ state are 1^{++} . These quantum numbers are consistent with those predicted by the molecular or tetraquark models and with the $\chi_{c1}(2^3P_1)$ charmonium state [32], possibly mixed with a molecule [10]. Other charmonium states are excluded. No significant D-wave fraction is found, with an upper limit of 4% at 95% C.L. The S-wave dominance is expected in the charmonium or tetraquark models, in which the $X(3872)$ state has a compact size. An extended size, such as that predicted by the molecular model, implies more favorable conditions for the D wave. However, conclusive discrimination among models is difficult because quantitative predictions are not available.

We express our gratitude to our colleagues in the CERN accelerator departments for the excellent performance of the LHC. We thank the technical and administrative staff at the LHCb institutes. We acknowledge support from CERN and from the national agencies: CAPES, CNPq, FAPERJ and FINEP (Brazil); NSFC (China); CNRS/IN2P3

PHYSICAL REVIEW D **92**, 011102(R) (2015)

(France); BMBF, DFG, HGF and MPG (Germany); INFN (Italy); FOM and NWO (The Netherlands); MNiSW and NCN (Poland); MEN/IFA (Romania); MinES and FANO (Russia); MinECo (Spain); SNSF and SER (Switzerland); NASU (Ukraine); STFC (United Kingdom); and NSF (U.S.). The Tier1 computing centers are supported by IN2P3 (France), KIT and BMBF (Germany), INFN (Italy), NWO and SURF (The Netherlands), PIC (Spain) and GridPP (United Kingdom). We are indebted to the communities behind the multiple open source software packages on which we depend. We are also thankful for the computing resources and the access to software research and development tools provided by Yandex LLC (Russia). Individual groups or members have received support from EPLANET, Marie Skłodowska-Curie Actions and ERC (European Union), Conseil général de Haute-Savoie, Labex ENIGMASS and OCEVU, Région Auvergne (France), RFBR (Russia), XuntaGal and GENCAT (Spain), Royal Society and Royal Commission for the Exhibition of 1851 (United Kingdom).

-
- [1] S.-K. Choi *et al.* (Belle Collaboration), *Phys. Rev. Lett.* **91**, 262001 (2003).
 - [2] D. Acosta *et al.* (CDF Collaboration), *Phys. Rev. Lett.* **93**, 072001 (2004).
 - [3] V. M. Abazov *et al.* (D0 Collaboration), *Phys. Rev. Lett.* **93**, 162002 (2004).
 - [4] B. Aubert *et al.* (BABAR Collaboration), *Phys. Rev. D* **71**, 071103 (2005).
 - [5] R. Aaij *et al.* (LHCb Collaboration), *Eur. Phys. J. C* **72**, 1972 (2012).
 - [6] S. Chatrchyan *et al.* (CMS Collaboration), *J. High Energy Phys.* **04** (2013) 154.
 - [7] K. A. Olive *et al.* (Particle Data Group), *Chin. Phys. C* **38**, 090001 (2014).
 - [8] N. A. Tornqvist, *Phys. Lett. B* **590**, 209 (2004).
 - [9] L. Maiani, F. Piccinini, A. D. Polosa, and V. Riquer, *Phys. Rev. D* **71**, 014028 (2005).
 - [10] C. Hanhart, Y. S. Kalashnikova, and A. V. Nefediev, *Eur. Phys. J. A* **47**, 101 (2011).
 - [11] B. Aubert *et al.* (BABAR Collaboration), *Phys. Rev. D* **74**, 071101 (2006).
 - [12] V. Bhardwaj *et al.* (Belle Collaboration), *Phys. Rev. Lett.* **107**, 091803 (2011).
 - [13] R. Aaij *et al.* (LHCb Collaboration), *Nucl. Phys.* **B886**, 665 (2014).
 - [14] S.-K. Choi *et al.* (Belle Collaboration), *Phys. Rev. D* **84**, 052004 (2011).
 - [15] A. Abulencia *et al.* (CDF Collaboration), *Phys. Rev. Lett.* **96**, 102002 (2006).
 - [16] A. Abulencia *et al.* (CDF Collaboration), *Phys. Rev. Lett.* **98**, 132002 (2007).
 - [17] R. Aaij *et al.* (LHCb Collaboration), *Phys. Rev. Lett.* **110**, 222001 (2013).
 - [18] A. A. Alves, Jr. *et al.* (LHCb Collaboration), *J. Instrum.* **3**, S08005 (2008).
 - [19] R. Aaij *et al.* (LHCb Collaboration), *Int. J. Mod. Phys. A* **30**, 1530022 (2015).
 - [20] T. Skwarnicki, Ph.D. thesis, Institute of Nuclear Physics of the Polish Academy of Sciences, 1986 [Deutsches Elektronen-Synchrotron Report No. DESY-F31-86-02, 1986 (unpublished)], <http://inspirehep.net/record/230779/files/230779.pdf>.
 - [21] M. Jacob and G. C. Wick, *Ann. Phys. (N.Y.)* **7**, 404 (1959).
 - [22] J. D. Richman, Report No. CALT-68-1148, 1984, <http://charm.physics.ucsb.edu/people/richman/ExperimentersGuideToTheHelicityFormalism.pdf>.
 - [23] S. U. Chung, *Phys. Rev. D* **57**, 431 (1998).
 - [24] T. Sjöstrand, S. Mrenna, and P. Skands, *J. High Energy Phys.* **05** (2006) 026.
 - [25] I. Belyaev *et al.*, in *Proceedings of the IEEE Nuclear Science Symposium Conference Record (NSS/MIC)*, Knoxville, TN, 2010 (IEEE, New York, 2011), p. 1155.
 - [26] D. J. Lange, *Nucl. Instrum. Methods Phys. Res., Sect. A* **462**, 152 (2001).
 - [27] J. Allison *et al.* (GEANT4 Collaboration), *IEEE Trans. Nucl. Sci.* **53**, 270 (2006); S. Agostinelli *et al.* (GEANT4 Collaboration), *Nucl. Instrum. Methods Phys. Res., Sect. A* **506**, 250 (2003).
 - [28] M. Clemencic, G. Corti, S. Easo, C. R. Jones, S. Miglioranzi, M. Pappagallo, and P. Robbe, *J. Phys. Conf. Ser.* **331**, 032023 (2011).

- [29] R. Aaij *et al.* (LHCb Collaboration), Phys. Rev. Lett. **113**, 162001 (2014).
- [30] R. Aaij *et al.* (LHCb Collaboration), Phys. Rev. D **90**, 072003 (2014).
- [31] M. Pivk and F. R. Le Diberder, Nucl. Instrum. Methods Phys. Res., Sect. A **555**, 356 (2005).
- [32] N. N. Achasov and E. V. Rogozina, $X(3872), I^G(J^{PC}) = 0^+(1^{++})$, as the $\chi_{1c}(2P)$ charmonium, arXiv:1501.03583.

- R. Aaij,³⁸ B. Adeva,³⁷ M. Adinolfi,⁴⁶ A. Affolder,⁵² Z. Ajaltouni,⁵ S. Akar,⁶ J. Albrecht,⁹ F. Alessio,³⁸ M. Alexander,⁵¹ S. Ali,⁴¹ G. Alkhazov,³⁰ P. Alvarez Cartelle,⁵³ A. A. Alves Jr.,⁵⁷ S. Amato,² S. Amerio,²² Y. Amhis,⁷ L. An,³ L. Anderlini,^{17,a} J. Anderson,⁴⁰ M. Andreotti,^{16,b} J. E. Andrews,⁵⁸ R. B. Appleby,⁵⁴ O. Aquines Gutierrez,¹⁰ F. Archilli,³⁸ P. d'Argent,¹¹ A. Artamonov,³⁵ M. Artuso,⁵⁹ E. Aslanides,⁶ G. Auriemma,^{25,c} M. Baalouch,⁵ S. Bachmann,¹¹ J. J. Back,⁴⁸ A. Badalov,³⁶ C. Baesso,⁶⁰ W. Baldini,^{16,38} R. J. Barlow,⁵⁴ C. Barschel,³⁸ S. Barsuk,⁷ W. Barter,³⁸ V. Batozskaya,²⁸ V. Battista,³⁹ A. Bay,³⁹ L. Beaucourt,⁴ J. Beddow,⁵¹ F. Bedeschi,²³ I. Bediaga,¹ L. J. Bel,⁴¹ I. Belyaev,³¹ E. Ben-Haim,⁸ G. Bencivenni,¹⁸ S. Benson,³⁸ J. Benton,⁴⁶ A. Berezhnoy,³² R. Bernet,⁴⁰ A. Bertolin,²² M.-O. Bettler,³⁸ M. van Beuzekom,⁴¹ A. Bien,¹¹ S. Bifani,⁴⁵ T. Bird,⁵⁴ A. Birnkraut,⁹ A. Bizzeti,^{17,d} T. Blake,⁴⁸ F. Blanc,³⁹ J. Blouw,¹⁰ S. Blusk,⁵⁹ V. Bocci,²⁵ A. Bondar,³⁴ N. Bondar,^{30,38} W. Bonivento,¹⁵ S. Borghi,⁵⁴ M. Borsato,⁷ T. J. V. Bowcock,⁵² E. Bowen,⁴⁰ C. Bozzi,¹⁶ S. Braun,¹¹ D. Brett,⁵⁴ M. Britsch,¹⁰ T. Britton,⁵⁹ J. Brodzicka,⁵⁴ N. H. Brook,⁴⁶ A. Bursche,⁴⁰ J. Buytaert,³⁸ S. Cadeddu,¹⁵ R. Calabrese,^{16,b} M. Calvi,^{20,e} M. Calvo Gomez,^{36,f} P. Campana,¹⁸ D. Campora Perez,³⁸ L. Capriotti,⁵⁴ A. Carbone,^{14,g} G. Carboni,^{24,h} R. Cardinale,^{19,i} A. Cardini,¹⁵ P. Carniti,²⁰ L. Carson,⁵⁰ K. Carvalho Akiba,^{2,38} R. Casanova Mohr,³⁶ G. Casse,⁵² L. Cassina,^{20,e} L. Castillo Garcia,³⁸ M. Cattaneo,³⁸ Ch. Cauet,⁹ G. Cavallero,¹⁹ R. Cenci,^{23,j} M. Charles,⁸ Ph. Charpentier,³⁸ M. Chefdeville,⁴ S. Chen,⁵⁴ S.-F. Cheung,⁵⁵ N. Chiapolini,⁴⁰ M. Chrzaszcz,^{40,26} X. Cid Vidal,³⁸ G. Ciezarek,⁴¹ P. E. L. Clarke,⁵⁰ M. Clemencic,³⁸ H. V. Cliff,⁴⁷ J. Closier,³⁸ V. Coco,³⁸ J. Cogan,⁶ E. Cogneras,⁵ V. Cogoni,^{15,k} L. Cojocariu,²⁹ G. Collazuol,²² P. Collins,³⁸ A. Comerma-Montells,¹¹ A. Contu,^{15,38} A. Cook,⁴⁶ M. Coombes,⁴⁶ S. Coquereau,⁸ G. Corti,³⁸ M. Corvo,^{16,b} B. Couturier,³⁸ G. A. Cowan,⁵⁰ D. C. Craik,⁴⁸ A. Crocombe,⁴⁸ M. Cruz Torres,⁶⁰ S. Cunliffe,⁵³ R. Currie,⁵³ C. D'Ambrosio,³⁸ J. Dalseno,⁴⁶ P. N. Y. David,⁴¹ A. Davis,⁵⁷ K. De Bruyn,⁴¹ S. De Capua,⁵⁴ M. De Cian,¹¹ J. M. De Miranda,¹ L. De Paula,² W. De Silva,⁵⁷ P. De Simone,¹⁸ C.-T. Dean,⁵¹ D. Decamp,⁴ M. Deckenhoff,⁹ L. Del Buono,⁸ N. Déléage,⁴ D. Derkach,⁵⁵ O. Deschamps,⁵ F. Dettori,³⁸ B. Dey,⁴⁰ A. Di Canto,³⁸ F. Di Ruscio,²⁴ H. Dijkstra,³⁸ S. Donleavy,⁵² F. Dordei,¹¹ M. Dorigo,³⁹ A. Dosil Suárez,³⁷ D. Dossett,⁴⁸ A. Dovbnya,⁴³ K. Dreimanis,⁵² L. Dufour,⁴¹ G. Dujany,⁵⁴ F. Dupertuis,³⁹ P. Durante,³⁸ R. Dzhelyadin,³⁵ A. Dziurda,²⁶ A. Dzyuba,³⁰ S. Easo,^{49,38} U. Egede,⁵³ V. Egorychev,³¹ S. Eidelman,³⁴ S. Eisenhardt,⁵⁰ U. Eitschberger,⁹ R. Ekelhof,⁹ L. Eklund,⁵¹ I. El Rifai,⁵ Ch. Elsasser,⁴⁰ S. Ely,⁵⁹ S. Esen,¹¹ H. M. Evans,⁴⁷ T. Evans,⁵⁵ A. Falabella,¹⁴ C. Färber,¹¹ C. Farinelli,⁴¹ N. Farley,⁴⁵ S. Farry,⁵² R. Fay,⁵² D. Ferguson,⁵⁰ V. Fernandez Albor,³⁷ F. Ferrari,¹⁴ F. Ferreira Rodrigues,¹ M. Ferro-Luzzi,³⁸ S. Filippov,³³ M. Fiore,^{16,38,b} M. Fiorini,^{16,b} M. Firlej,²⁷ C. Fitzpatrick,³⁹ T. Fiutowski,²⁷ P. Fol,⁵³ M. Fontana,¹⁰ F. Fontanelli,^{19,i} R. Forty,³⁸ O. Francisco,² M. Frank,³⁸ C. Frei,³⁸ M. Frosini,¹⁷ J. Fu,²¹ E. Furfaro,^{24,h} A. Gallas Torreira,³⁷ D. Galli,^{14,g} S. Gallorini,^{22,38} S. Gambetta,^{19,i} M. Gandelman,² P. Gandini,⁵⁵ Y. Gao,³ J. García Pardiñas,³⁷ J. Garofoli,⁵⁹ J. Garra Tico,⁴⁷ L. Garrido,³⁶ D. Gascon,³⁶ C. Gaspar,³⁸ U. Gastaldi,¹⁶ R. Gauld,⁵⁵ L. Gavardi,⁹ G. Gazzoni,⁵ A. Geraci,^{21,l} D. Gerick,¹¹ E. Gersabeck,¹¹ M. Gersabeck,⁵⁴ T. Gershon,⁴⁸ Ph. Ghez,⁴ A. Gianelle,²² S. Giani,³⁹ V. Gibson,⁴⁷ L. Giubega,²⁹ V. V. Gligorov,³⁸ C. Göbel,⁶⁰ D. Golubkov,³¹ A. Golutvin,^{53,31,38} A. Gomes,^{1,m} C. Gotti,^{20,e} M. Grabalosa Gándara,⁵ R. Graciani Diaz,³⁶ L. A. Granado Cardoso,³⁸ E. Graugés,³⁶ E. Graverini,⁴⁰ G. Graziani,¹⁷ A. Grecu,²⁹ E. Greening,⁵⁵ S. Gregson,⁴⁷ P. Griffith,⁴⁵ L. Grillo,¹¹ O. Grünberg,⁶³ B. Gui,⁵⁹ E. Gushchin,³³ Yu. Guz,^{35,38} T. Gys,³⁸ C. Hadjivasiliou,⁵⁹ G. Haefeli,³⁹ C. Haen,³⁸ S. C. Haines,⁴⁷ S. Hall,⁵³ B. Hamilton,⁵⁸ T. Hampson,⁴⁶ X. Han,¹¹ S. Hansmann-Menzemer,¹¹ N. Harnew,⁵⁵ S. T. Harnew,⁴⁶ J. Harrison,⁵⁴ J. He,³⁸ T. Head,³⁹ V. Heijne,⁴¹ K. Hennessy,⁵² P. Henrard,⁵ L. Henry,⁸ J. A. Hernando Morata,³⁷ E. van Herwijnen,³⁸ M. Heß,⁶³ A. Hicheur,² D. Hill,⁵⁵ M. Hoballah,⁵ C. Hombach,⁵⁴ W. Hulsbergen,⁴¹ T. Humair,⁵³ N. Hussain,⁵⁵ D. Hutchcroft,⁵² D. Hynds,⁵¹ M. Idzik,²⁷ P. Ilten,⁵⁶ R. Jacobsson,³⁸ A. Jaeger,¹¹ J. Jalocha,⁵⁵ E. Jans,⁴¹ A. Jawahery,⁵⁸ F. Jing,³ M. John,⁵⁵ D. Johnson,³⁸ C. R. Jones,⁴⁷ C. Joram,³⁸ B. Jost,³⁸ N. Jurik,⁵⁹ S. Kandybei,⁴³ W. Kanso,⁶ M. Karacson,³⁸ T. M. Karbach,^{38,†} S. Karodia,⁵¹ M. Kelsey,⁵⁹ I. R. Kenyon,⁴⁵ M. Kenzie,³⁸ T. Ketel,⁴² B. Khanji,^{20,38,e} C. Khurewathanakul,³⁹ S. Klaver,⁵⁴ K. Klimaszewski,²⁸ O. Kochebina,⁷ M. Kolpin,¹¹ I. Komarov,³⁹ R. F. Koopman,⁴² P. Koppenburg,^{41,38} M. Korolev,³² L. Kravchuk,³³ K. Kreplin,¹¹ M. Kreps,⁴⁸ G. Krocker,¹¹

- P. Krovovny,³⁴ F. Kruse,⁹ W. Kucewicz,^{26,n} M. Kucharczyk,²⁶ V. Kudryavtsev,³⁴ K. Kurek,²⁸ T. Kvaratskheliya,³¹ V. N. La Thi,³⁹ D. Lacarrere,³⁸ G. Lafferty,⁵⁴ A. Lai,¹⁵ D. Lambert,⁵⁰ R. W. Lambert,⁴² G. Lanfranchi,¹⁸ C. Langenbruch,⁴⁸ B. Langhans,³⁸ T. Latham,⁴⁸ C. Lazzeroni,⁴⁵ R. Le Gac,⁶ J. van Leerdaam,⁴¹ J.-P. Lees,⁴ R. Lefèvre,⁵ A. Leflat,³² J. Lefrançois,⁷ O. Leroy,⁶ T. Lesiak,²⁶ B. Leverington,¹¹ Y. Li,⁷ T. Likhomanenko,^{65,64} M. Liles,⁵² R. Lindner,³⁸ C. Linn,³⁸ F. Lionetto,⁴⁰ B. Liu,¹⁵ S. Lohn,³⁸ I. Longstaff,⁵¹ J. H. Lopes,² P. Lowdon,⁴⁰ D. Lucchesi,^{22,o} H. Luo,⁵⁰ A. Lupato,²² E. Luppi,^{16,b} O. Lupton,⁵⁵ F. Machefert,⁷ F. Maciuc,²⁹ O. Maev,³⁰ K. Maguire,⁵⁴ S. Malde,⁵⁵ A. Malinin,⁶⁴ G. Manca,^{15,k} G. Mancinelli,⁶ P. Manning,⁵⁹ A. Mapelli,³⁸ J. Maratas,⁵ J. F. Marchand,⁴ U. Marconi,¹⁴ C. Marin Benito,³⁶ P. Marino,^{23,38,j} R. Märki,³⁹ J. Marks,¹¹ G. Martellotti,²⁵ M. Martinelli,³⁹ D. Martinez Santos,⁴² F. Martinez Vidal,⁶⁶ D. Martins Tostes,² A. Massafferri,¹ R. Matev,³⁸ A. Mathad,⁴⁸ Z. Mathe,³⁸ C. Matteuzzi,²⁰ A. Mauri,⁴⁰ B. Maurin,³⁹ A. Mazurov,⁴⁵ M. McCann,⁵³ J. McCarthy,⁴⁵ A. McNab,⁵⁴ R. McNulty,¹² B. Meadows,⁵⁷ F. Meier,⁹ M. Meissner,¹¹ M. Merk,⁴¹ D. A. Milanes,⁶² M.-N. Minard,⁴ D. S. Mitzel,¹¹ J. Molina Rodriguez,⁶⁰ S. Monteil,⁵ M. Morandin,²² P. Morawski,²⁷ A. Mordà,⁶ M. J. Morello,^{23,j} J. Moron,²⁷ A. B. Morris,⁵⁰ R. Mountain,⁵⁹ F. Muheim,⁵⁰ J. Müller,⁹ K. Müller,⁴⁰ V. Müller,⁹ M. Mussini,¹⁴ B. Muster,³⁹ P. Naik,⁴⁶ T. Nakada,³⁹ R. Nandakumar,⁴⁹ I. Nasteva,² M. Needham,⁵⁰ N. Neri,²¹ S. Neubert,¹¹ N. Neufeld,³⁸ M. Neuner,¹¹ A. D. Nguyen,³⁹ T. D. Nguyen,³⁹ C. Nguyen-Mau,^{39,p} V. Niess,⁵ R. Niet,⁹ N. Nikitin,³² T. Nikodem,¹¹ D. Ninci,²³ A. Novoselov,³⁵ D. P. O'Hanlon,⁴⁸ A. Oblakowska-Mucha,²⁷ V. Obraztsov,³⁵ S. Ogilvy,⁵¹ O. Okhrimenko,⁴⁴ R. Oldeman,^{15,k} C. J. G. Onderwater,⁶⁷ B. Osorio Rodrigues,¹ J. M. Otalora Goicochea,² A. Otto,³⁸ P. Owen,⁵³ A. Oyanguren,⁶⁶ A. Palano,^{13,q} F. Palombo,^{21,r} M. Palutan,¹⁸ J. Panman,³⁸ A. Papanestis,⁴⁹ M. Pappagallo,⁵¹ L. L. Pappalardo,^{16,b} C. Parkes,⁵⁴ G. Passaleva,¹⁷ G. D. Patel,⁵² M. Patel,⁵³ C. Patrignani,^{19,i} A. Pearce,^{54,49} A. Pellegrino,⁴¹ G. Penso,^{25,s} M. Pepe Altarelli,³⁸ S. Perazzini,^{14,g} P. Perret,⁵ L. Pescatore,⁴⁵ K. Petridis,⁴⁶ A. Petrolini,^{19,i} M. Petruzzo,²¹ E. Picatoste Olloqui,³⁶ B. Pietrzyk,⁴ T. Pilař,⁴⁸ D. Pinci,²⁵ A. Pistone,¹⁹ S. Playfer,⁵⁰ M. Plo Casasus,³⁷ T. Poikela,³⁸ F. Polci,⁸ A. Poluektov,^{48,34} I. Polyakov,³¹ E. Polycarpo,² A. Popov,³⁵ D. Popov,¹⁰ B. Popovici,²⁹ C. Potterat,² E. Price,⁴⁶ J. D. Price,⁵² J. Prisciandaro,³⁹ A. Pritchard,⁵² C. Prouve,⁴⁶ V. Pugatch,⁴⁴ A. Puig Navarro,³⁹ G. Punzi,^{23,t} W. Qian,⁴ R. Quagliani,^{7,46} B. Rachwal,²⁶ J. H. Rademacker,⁴⁶ B. Rakotomiaramanana,³⁹ M. Rama,²³ M. S. Rangel,² I. Raniuk,⁴³ N. Rauschmayr,³⁸ G. Raven,⁴² F. Redi,⁵³ S. Reichert,⁵⁴ M. M. Reid,⁴⁸ A. C. dos Reis,¹ S. Ricciardi,⁴⁹ S. Richards,⁴⁶ M. Rihl,³⁸ K. Rinnert,⁵² V. Rives Molina,³⁶ P. Robbe,^{7,38} A. B. Rodrigues,¹ E. Rodrigues,⁵⁴ J. A. Rodriguez Lopez,⁶² P. Rodriguez Perez,⁵⁴ S. Roiser,³⁸ V. Romanovsky,³⁵ A. Romero Vidal,³⁷ M. Rotondo,²² J. Rouvinet,³⁹ T. Ruf,³⁸ H. Ruiz,³⁶ P. Ruiz Valls,⁶⁶ J. J. Saborido Silva,³⁷ N. Sagidova,³⁰ P. Sail,⁵¹ B. Saitta,^{15,k} V. Salustino Guimaraes,² C. Sanchez Mayordomo,⁶⁶ B. Sanmartin Sedes,³⁷ R. Santacesaria,²⁵ C. Santamarina Rios,³⁷ M. Santimaria,¹⁸ E. Santovetti,^{24,h} A. Sarti,^{18,s} C. Satriano,^{25,c} A. Satta,²⁴ D. M. Saunders,⁴⁶ D. Savrina,^{31,32} M. Schiller,³⁸ H. Schindler,³⁸ M. Schlupp,⁹ M. Schmelling,¹⁰ T. Schmelzer,⁹ B. Schmidt,³⁸ O. Schneider,³⁹ A. Schopper,³⁸ M.-H. Schune,⁷ R. Schwemmer,³⁸ B. Sciascia,¹⁸ A. Sciubba,^{25,s} A. Semennikov,³¹ I. Sepp,⁵³ N. Serra,⁴⁰ J. Serrano,⁶ L. Sestini,²² P. Seyfert,¹¹ M. Shapkin,³⁵ I. Shapoval,^{16,43,b} Y. Shcheglov,³⁰ T. Shears,⁵² L. Shekhtman,³⁴ V. Shevchenko,⁶⁴ A. Shires,⁹ R. Silva Coutinho,⁴⁸ G. Simi,²² M. Sirendi,⁴⁷ N. Skidmore,⁴⁶ I. Skillicorn,⁵¹ T. Skwarnicki,⁵⁹ E. Smith,^{55,49} E. Smith,⁵³ J. Smith,⁴⁷ M. Smith,⁵⁴ H. Snoek,⁴¹ M. D. Sokoloff,^{57,38} F. J. P. Soler,⁵¹ F. Soomro,³⁹ D. Souza,⁴⁶ B. Souza De Paula,² B. Spaan,⁹ P. Spradlin,⁵¹ S. Sridharan,³⁸ F. Stagni,³⁸ M. Stahl,¹¹ S. Stahl,³⁸ O. Steinkamp,⁴⁰ O. Stenyakin,³⁵ F. Sterpka,⁵⁹ S. Stevenson,⁵⁵ S. Stoica,²⁹ S. Stone,⁵⁹ B. Storaci,⁴⁰ S. Stracka,^{23,j} M. Stratifici,²⁹ U. Straumann,⁴⁰ R. Stroili,²² L. Sun,⁵⁷ W. Sutcliffe,⁵³ K. Swientek,²⁷ S. Swientek,⁹ V. Syropoulos,⁴² M. Szczekowski,²⁸ P. Szczypka,^{39,38} T. Szumlak,²⁷ S. T'Jampens,⁴ T. Tekampe,⁹ M. Teklichyn,⁷ G. Tellarini,^{16,b} F. Teubert,³⁸ C. Thomas,⁵⁵ E. Thomas,³⁸ J. van Tilburg,⁴¹ V. Tisserand,⁴ M. Tobin,³⁹ J. Todd,⁵⁷ S. Tolk,⁴² L. Tomassetti,^{16,b} D. Tonelli,³⁸ S. Topp-Joergensen,⁵⁵ N. Torr,⁵⁵ E. Tournefier,⁴ S. Tourneur,³⁹ K. Trabelsi,³⁹ M. T. Tran,³⁹ M. Tresch,⁴⁰ A. Trisovic,³⁸ A. Tsaregorodtsev,⁶ P. Tsopelas,⁴¹ N. Tuning,^{41,38} A. Ukleja,²⁸ A. Ustyuzhanin,^{65,64} U. Uwer,¹¹ C. Vacca,^{15,k} V. Vagnoni,¹⁴ G. Valenti,¹⁴ A. Vallier,⁷ R. Vazquez Gomez,¹⁸ P. Vazquez Regueiro,³⁷ C. Vázquez Sierra,³⁷ S. Vecchi,¹⁶ J. J. Velthuis,⁴⁶ M. Veltri,^{17,u} G. Veneziano,³⁹ M. Vesterinen,¹¹ B. Viaud,⁷ D. Vieira,² M. Vieites Diaz,³⁷ X. Vilasis-Cardona,^{36,f} A. Vollhardt,⁴⁰ D. Volyansky,¹⁰ D. Voong,⁴⁶ A. Vorobyev,³⁰ V. Vorobyev,³⁴ C. Voß,⁶³ J. A. de Vries,⁴¹ R. Waldi,⁶³ C. Wallace,⁴⁸ R. Wallace,¹² J. Walsh,²³ S. Wandernoth,¹¹ J. Wang,⁵⁹ D. R. Ward,⁴⁷ N. K. Watson,⁴⁵ D. Websdale,⁵³ A. Weiden,⁴⁰ M. Whitehead,⁴⁸ D. Wiedner,¹¹ G. Wilkinson,^{55,38} M. Wilkinson,⁵⁹ M. Williams,³⁸ M. P. Williams,⁴⁵ M. Williams,⁵⁶ F. F. Wilson,⁴⁹ J. Wimberley,⁵⁸ J. Wishahi,⁹ W. Wislicki,²⁸ M. Witek,²⁶ G. Wormser,⁷ S. A. Wotton,⁴⁷ S. Wright,⁴⁷ K. Wyllie,³⁸ Y. Xie,⁶¹ Z. Xu,³⁹ Z. Yang,³

X. Yuan,³⁴ O. Yushchenko,³⁵ M. Zangoli,¹⁴ M. Zavertyaev,^{10,v} L. Zhang,³ Y. Zhang,³
A. Zhelezov,¹¹ A. Zhokhov,³¹ and L. Zhong³

(LHCb Collaboration)

¹*Centro Brasileiro de Pesquisas Físicas (CBPF), Rio de Janeiro, Brazil*

²*Universidade Federal do Rio de Janeiro (UFRJ), Rio de Janeiro, Brazil*

³*Center for High Energy Physics, Tsinghua University, Beijing, China*

⁴*LAPP, Université Savoie Mont-Blanc, CNRS/IN2P3, Annecy-Le-Vieux, France*

⁵*Clermont Université, Université Blaise Pascal, CNRS/IN2P3, LPC, Clermont-Ferrand, France*

⁶*CPPM, Aix-Marseille Université, CNRS/IN2P3, Marseille, France*

⁷*LAL, Université Paris-Sud, CNRS/IN2P3, Orsay, France*

⁸*LPNHE, Université Pierre et Marie Curie, Université Paris Diderot, CNRS/IN2P3, Paris, France*

⁹*Fakultät Physik, Technische Universität Dortmund, Dortmund, Germany*

¹⁰*Max-Planck-Institut für Kernphysik (MPIK), Heidelberg, Germany*

¹¹*Physikalisches Institut, Ruprecht-Karls-Universität Heidelberg, Heidelberg, Germany*

¹²*School of Physics, University College Dublin, Dublin, Ireland*

¹³*Sezione INFN di Bari, Bari, Italy*

¹⁴*Sezione INFN di Bologna, Bologna, Italy*

¹⁵*Sezione INFN di Cagliari, Cagliari, Italy*

¹⁶*Sezione INFN di Ferrara, Ferrara, Italy*

¹⁷*Sezione INFN di Firenze, Firenze, Italy*

¹⁸*Laboratori Nazionali dell'INFN di Frascati, Frascati, Italy*

¹⁹*Sezione INFN di Genova, Genova, Italy*

²⁰*Sezione INFN di Milano Bicocca, Milano, Italy*

²¹*Sezione INFN di Milano, Milano, Italy*

²²*Sezione INFN di Padova, Padova, Italy*

²³*Sezione INFN di Pisa, Pisa, Italy*

²⁴*Sezione INFN di Roma Tor Vergata, Roma, Italy*

²⁵*Sezione INFN di Roma La Sapienza, Roma, Italy*

²⁶*Henryk Niewodniczanski Institute of Nuclear Physics Polish Academy of Sciences, Kraków, Poland*

²⁷*AGH - University of Science and Technology, Faculty of Physics and Applied Computer Science, Kraków, Poland*

²⁸*National Center for Nuclear Research (NCBJ), Warsaw, Poland*

²⁹*Horia Hulubei National Institute of Physics and Nuclear Engineering, Bucharest-Magurele, Romania*

³⁰*Petersburg Nuclear Physics Institute (PNPI), Gatchina, Russia*

³¹*Institute of Theoretical and Experimental Physics (ITEP), Moscow, Russia*

³²*Institute of Nuclear Physics, Moscow State University (SINP MSU), Moscow, Russia*

³³*Institute for Nuclear Research of the Russian Academy of Sciences (INR RAN), Moscow, Russia*

³⁴*Budker Institute of Nuclear Physics (SB RAS) and Novosibirsk State University, Novosibirsk, Russia*

³⁵*Institute for High Energy Physics (IHEP), Protvino, Russia*

³⁶*Universitat de Barcelona, Barcelona, Spain*

³⁷*Universidad de Santiago de Compostela, Santiago de Compostela, Spain*

³⁸*European Organization for Nuclear Research (CERN), Geneva, Switzerland*

³⁹*Ecole Polytechnique Fédérale de Lausanne (EPFL), Lausanne, Switzerland*

⁴⁰*Physik-Institut, Universität Zürich, Zürich, Switzerland*

⁴¹*Nikhef National Institute for Subatomic Physics, Amsterdam, The Netherlands*

⁴²*Nikhef National Institute for Subatomic Physics and VU University Amsterdam, Amsterdam, The Netherlands*

⁴³*NSC Kharkiv Institute of Physics and Technology (NSC KIPT), Kharkiv, Ukraine*

⁴⁴*Institute for Nuclear Research of the National Academy of Sciences (KINR), Kyiv, Ukraine*

⁴⁵*University of Birmingham, Birmingham, United Kingdom*

⁴⁶*H.H. Wills Physics Laboratory, University of Bristol, Bristol, United Kingdom*

⁴⁷*Cavendish Laboratory, University of Cambridge, Cambridge, United Kingdom*

⁴⁸*Department of Physics, University of Warwick, Coventry, United Kingdom*

⁴⁹*STFC Rutherford Appleton Laboratory, Didcot, United Kingdom*

⁵⁰*School of Physics and Astronomy, University of Edinburgh, Edinburgh, United Kingdom*

⁵¹*School of Physics and Astronomy, University of Glasgow, Glasgow, United Kingdom*

⁵²*Oliver Lodge Laboratory, University of Liverpool, Liverpool, United Kingdom*

⁵³*Imperial College London, London, United Kingdom*⁵⁴*School of Physics and Astronomy, University of Manchester, Manchester, United Kingdom*⁵⁵*Department of Physics, University of Oxford, Oxford, United Kingdom*⁵⁶*Massachusetts Institute of Technology, Cambridge, MA, United States*⁵⁷*University of Cincinnati, Cincinnati, OH, United States*⁵⁸*University of Maryland, College Park, MD, United States*⁵⁹*Syracuse University, Syracuse, NY, United States*⁶⁰*Pontifícia Universidade Católica do Rio de Janeiro (PUC-Rio), Rio de Janeiro, Brazil**(associated with Universidade Federal do Rio de Janeiro (UFRJ), Rio de Janeiro, Brazil)*⁶¹*Institute of Particle Physics, Central China Normal University, Wuhan, Hubei, China**(associated with Center for High Energy Physics, Tsinghua University, Beijing, China)*⁶²*Departamento de Física, Universidad Nacional de Colombia, Bogota, Colombia (associated with LPNHE, Université Pierre et Marie Curie, Université Paris Diderot, CNRS/IN2P3, Paris, France)*⁶³*Institut für Physik, Universität Rostock, Rostock, Germany (associated with Physikalisches Institut, Ruprecht-Karls-Universität Heidelberg, Heidelberg, Germany)*⁶⁴*National Research Centre Kurchatov Institute, Moscow, Russia (associated with Institute of Theoretical and Experimental Physics (ITEP), Moscow, Russia)*⁶⁵*Yandex School of Data Analysis, Moscow, Russia (associated with Institute of Theoretical and Experimental Physics (ITEP), Moscow, Russia)*⁶⁶*Instituto de Física Corpuscular (IFIC), Universitat de Valencia-CSIC, Valencia, Spain
(associated with Universitat de Barcelona, Barcelona, Spain)*⁶⁷*Van Swinderen Institute, University of Groningen, Groningen, The Netherlands
(associated with Nikhef National Institute for Subatomic Physics, Amsterdam, The Netherlands)*[†]Deceased.^aAlso at Università di Firenze, Firenze, Italy^bAlso at Università di Ferrara, Ferrara, Italy^cAlso at Università della Basilicata, Potenza, Italy^dAlso at Università di Modena e Reggio Emilia, Modena, Italy^eAlso at Università di Milano Bicocca, Milano, Italy^fAlso at LIFAELS, La Salle, Universitat Ramon Llull, Barcelona, Spain^gAlso at Università di Bologna, Bologna, Italy^hAlso at Università di Roma Tor Vergata, Roma, ItalyⁱAlso at Università di Genova, Genova, Italy^jAlso at Scuola Normale Superiore, Pisa, Italy^kAlso at Università di Cagliari, Cagliari, Italy^lAlso at Politecnico di Milano, Milano, Italy^mAlso at Universidade Federal do Triângulo Mineiro (UFTM), Uberaba-MG, BrazilⁿAlso at AGH - University of Science and Technology, Faculty of Computer Science, Electronics and Telecommunications, Kraków, Poland^oAlso at Università di Padova, Padova, Italy^pAlso at Hanoi University of Science, Hanoi, Viet Nam^qAlso at Università di Bari, Bari, Italy^rAlso at Università degli Studi di Milano, Milano, Italy^sAlso at Università di Roma La Sapienza, Roma, Italy^tAlso at Università di Pisa, Pisa, Italy^uAlso at Università di Urbino, Urbino, Italy^vAlso at P.N. Lebedev Physical Institute, Russian Academy of Science (LPI RAS), Moscow, Russia